JOURNAL OF INFORMATION SCIENCE AND ENGINEERING 37, 733-752 (2021)
DOI: 10.6688/JISE.202107_37(4).0001

Radar Automatic Target Recognition Based on Real-Life HRRP of Ship Target by Using Convolutional Neural Network*

TSUNG-PIN CHEN[1], CHIH-LUNG LIN[2], KUO-CHIN FAN[1], WAN-YU LIN[1] AND CHIAO-WEN KAO[3]

[1]*Department of Computer Science and Information Engineering*
National Central University
Taoyuan City, 320 Taiwan
[2]*Graduate Institute of Intelligent Robotics*
Hwa Hsia University of Technology
New Taipei City, 235 Taiwan
[3]*Department of Economics and Finance*
Ming Chung University
Taoyuan City, 333 Taiwan
E-mail: {justin63.chen; linclr; kcfan.ncu; kitty60823; chiaowenk}@gmail.com

High-resolution range profile (HRRP) is one of the most important approaches for radar automatic target recognition (RATR), which can project the target echoes from the scattering center of a ship target onto the radar line of sight (RLOS). This paper proposes an approach to use convolutional neural networks (CNNs) to recognize HRRP ship targets and a two-dimensional HRRP data format as the input of the CNN network. Compared with traditional pattern recognition approaches of handcrafted features based on researchers' prior knowledge and experience, the target recognition approach with deep neural network helps to avoid excessive use of artificially designed rules to extract features, and deep learning can automatically get the deep description features of the target. The approach presented in this paper has three main advantages: (1) Experiments conducted on the ship's HRRP dataset collected from the actual coastline are more realistic than most other papers using simulated datasets; (2) Proposed two-dimensional binary-map HRRP data format has good recognition performance, so it can be known that proper data preprocessing can improve recognition accuracy; (3) It can be seen from the experimental results that the CNN-based method proves that CNN can automatically learn the discriminative deep features of HRRP. It is feasible to use CNN to radar automatic target recognition based on real-life radar HRRP of ship targets.

Keywords: high-resolution range profile (HRRP), convolutional neural network (CNN), radar automatic target recognition (RATR), artificial intelligence (AI), machine learning, radar line of sight (RLOS), automatic identification system (AIS), range-azimuth map (R-A map)

1. INTRODUCTION

Radar automatic target recognition (RATR) means that the radar antenna receives robust radar information from the radar microwave signal reflected from the target, and uses this information to automatically recognize the target. RATR technology has played an important role in modern coastal warning control, maritime rescue, navigation management and naval warfare, and has led to extensive research in the past few decades. In these studies, radar high-resolution range profile (HRRP) information for RATR is a promising technology.

Received September 10, 2020; revised December 15, 2020; accepted March 3, 2021.
Communicated by Ching-Chun Huang.
* This work was supported by the research granted from Ministry of Science and Technology (MOST 109-2637-E-146-001).

The radar HRRP is the one-dimensional projection of the target in the radar observation direction obtained by radar which reflects the energy distribution of the target scattering echoes in each range cell along the radar line of sight (RLOS) and implies information about the target geometry that contributes to the classification. In addition, it has relatively small data. Therefore, RATR based on HRRP has been widely concerned by experts and scholars engaged in radar automatic target recognition research. The most popular type of radar is the pulsed radar. The pulse repetition interval (PRI) is the time interval between two adjacent pulses. Each echo reflected by the target will generate a corresponding HRRP within the PRI. The radar HRRP of a ship target is shown in Fig. 1.

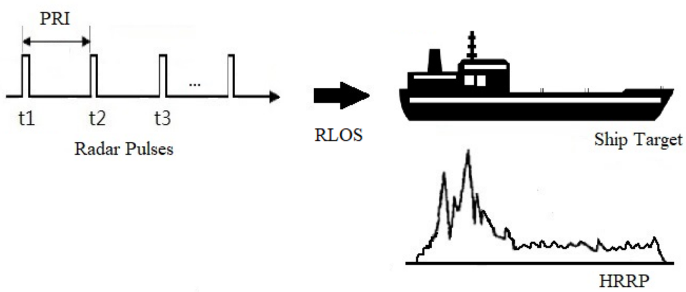

Fig. 1. Schematic diagram of radar HRRP for ship targets.

H.-J. Li and S.-H. Yang [1] used HRRP as the data feature vector and established decision rules to identify five types of aircraft based on matching scores. Y. Wang *et al.* [2] introduced atomic norm minimization to estimate the scattering center of HRRP to alleviate off-grid problems caused by traditional sparse inverse approaches. D. Zhou, X. Shen and W. Yang [3] proposed a radar target recognition fuzzy optimization transform approach based on HRRP. The goal of this approach is to maximize the distance between classes while preserving the within-class structure. J. Liu *et al.* [4] introduced a scale space theory to extract range profiles' multi-scale features. Although the structural features have excellent performance in RATR based on HRRP, they also indicate that the classification method still has the ameliorative possibility from the combination with other feature extraction techniques. D. Zhou [5] proposed a radar HRRP dictionary learning algorithm, namely reconstructive and discriminant dictionary learning algorithm based on sparse representation classification criteria. Extensive experimental results show that the algorithm is more robust to the variation of target aspect and noise's effect and superior to other similar approaches. L. Du *et al.* [6] introduced a novel noise-robust recognition method for HRRP data to enhance its recognition performance under the test condition of low signal-to-noise ratio (SNR). A. Zyweck and R. E. Bogner [7] proposed data preprocessing and subspace algorithms for HRRP recognition.

In the above approaches, feature extraction is the most critical step. Most of the radar dynamic target features are based on the domain knowledge of HRRP data, such as subspace features, high-order spectral features and differential power spectrum features. These features are artificially extracted, and the effect depends on the actual experience of the researchers and application background.

In recent years, with the rise of large-scale deep neural networks and the support of high-performance computing hardware, neural network deep learning technology has opened up a new research opportunity for the traditional radar automatic target recognition field. Therefore, some researchers began to use the high-dimensional nonlinear computing methods to pursue higher, more accurate and more robust type recognition performance.

J. Lundén and V. Koivunen [8] used the CNN to automatically extract features of HRRP targets from multiple static radar systems for target recognition. The experimental results show that the proposed approach can obtain good recognition performance even at low SNR, which is better than some traditional pattern recognition approaches. Therefore, the convolutional neural network is used to replace the traditional approach to identify the target.

The Hidden Markov model (HMM) is another widely discussed approach for realizing RATR using HRRP. B. Pei and Z. Bao [9] used hidden Markov model (HMM)-based method for recognizing HRRP by combining the location information of points scattering. B. Feng, B. Chen, and H. Liu [10] proposed a deep network with HRRP target recognition by adopting multi-layered nonlinear networks for feature learning, and established an effective loss function approach under Mahalanobis distance criterion. J. Lu *et al.* [11] proposed Fourier-Mellin transform (FMT) to eliminate the time-shift and azimuth dependence of radar signals, and used a binary tree-based multiclass support vector machine (SVM) for classification. J. Lu *et al.* [12] used Kolmogorov-smirnov test (KS test) to achieve frame segmentation, so that each frame of data satisfies the same Gaussian distribution, and different frame data meet different requirements distributed. Finally, based on the complex Gaussian distribution of ship identification, Bayesian classifiers are classified using traditional classifiers: support vector machines and Naive Bayes.

O. Karabayır *et al.* [13] used CNN for ship classification by stacking each one-dimensional HRRP into a two-dimensional gray-scale map, that is, copying 32 times 1×168 size one-dimensional HRRP into a 32×168 data image. J. Song *et al.* [14] proposed a multichannel CNN architecture for ground target HRRP recognition. This architecture can be applied to many forms of HRRP, such as real, complex, spectrum, polarization, and sequence. Compared with the single-channel form, the proposed method shows a considerable improvement in recognition accuracy.

Q. Zhang *et al.* [15] proposed a CNN-ELM network structure that combines convolutional neural networks with extreme learning machines for ship HRRP target recognition. The input HRRP data of the network will be reordered to convert one-dimensional data into two-dimensional data. In the experiment, the recognition rate of CNN-ELM reached 99.50%.

W. Jinwei *et al.* [16] proposed a CNN-BiRNN-based method to identify aircraft HRRP. The main contribution of this method is to use CNN to explore the spatial correlation of the raw HRRP data, extract the expression features, and then combine BiRNN to fully consider the time dependence between distance units. It is seen in the experiment that the best recognition effect of CNN-BiRNN reaches 93.30%.

The authors proposed a method in CVGIP 2020 [17], which applies CNN to HRRP of ship target recognition, and proves that an effective HRRP data format as the input of the CNN network can have good recognition accuracy. In this paper, the authors will give a more detailed description of how to build a real-life HRRP database with the help of automatic identification system (AIS). In addition, the authors have also done more experiments and data analysis to make this research more complete.

In summary, compared with traditional pattern recognition approaches based on hand-crafted features, the target recognition approach with deep neural network helps to avoid excessive use of artificially designed rules to extract features, and deep learning can automatically get the deep description features of the target. The features extracted by deep learning approach are more conducive to classification. Therefore, this research applies deep convolutional neural network to RATR by using real-life radar HRRP and obtains a good performance.

Fig. 2 shows the function blocks of the proposed approach. Firstly, the HRRP data are collected and labeled by manual. Then, the HRRP chips are cut as many frames with a designed frame-cutting software, construct the HRRP original database of the six types of targets. Secondly, some pre-processing of the signal is performed. The echo signal of the radar is first processed by non-coherent integration (NCI) to alleviate the fluctuation of the signal and increase SNR. Since the ship target has a certain reasonable size range, we eliminate noisy range cells to reduce the amount of data processing. Thirdly, according to the planned HRRP raw data format, three different HRRP data formats are generated as the subsequent input of CNNs. Finally, use three different data formats as the input of four different CNN architectures to explore which network architecture and data format can get the best recognition accuracy. Experimental results show that the proposed approach is comparable to the other state-of-the-art HRRP target recognition approaches.

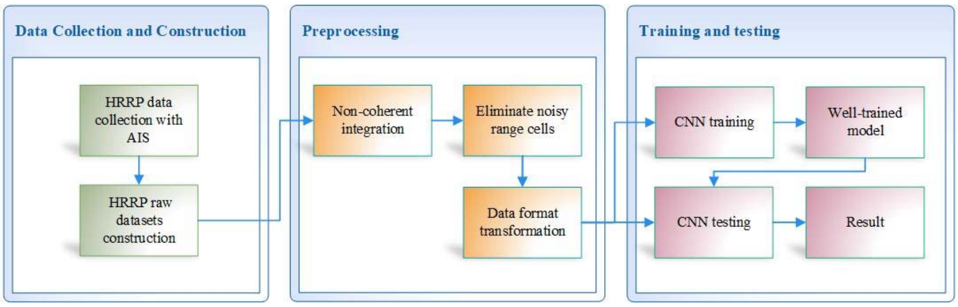

Fig. 2. The function blocks of the proposed approach.

The remainder of this paper is presented as follows. Section 2 describes the collection and construction of the ship HRRP dataset. Section 3 describes the procedures for preprocessing the HRRP of ship targets. The design of the proposed CNNs is presented in Section 4. The experimental results and analysis are illustrated in Section 5. Finally, the conclusions are described in Section 6.

2. COLLECTION AND CONSTRUCTION OF DATASET

The radar HRRPs used to recognize ship targets is carried out through ship information collected by radar and AIS. AIS is an automatic tracking system designed to provide information about ships, such as unique identification, position, course and speed, to facilitate maritime tracking and surveillance of ships. AIS information is complementary to maritime radar, which is still the primary method to avoid collisions for water transport.

The construction of the HRRP dataset follows four main steps. First, collect HRRP data of ships through radar. Next, the collected HRRP data are manually identified and labelled by using AIS information. Then, the HRRP chips are cut as many frames with a designed frame-cutting software. Finally, post-processing is done to each ship HRRP chip so as to guarantee the reliability and good quality. The HRRP ships dataset constructed by ourselves has three essential properties: reality, diversity and large scale.

The steps to collect HRRP data for ships are as follows. Firstly, use GPS to locate the radar equipment position. Secondly, turn on the radar and connect a notebook or handheld device to the AIS on internet to query current ship information near the coast and calculate search command parameters, including range-center, range-coverage, azimuth-center and azimuth-coverage. Thirdly, run the Range-Azimuth map (R-A map) software, as shown in Fig. 3.

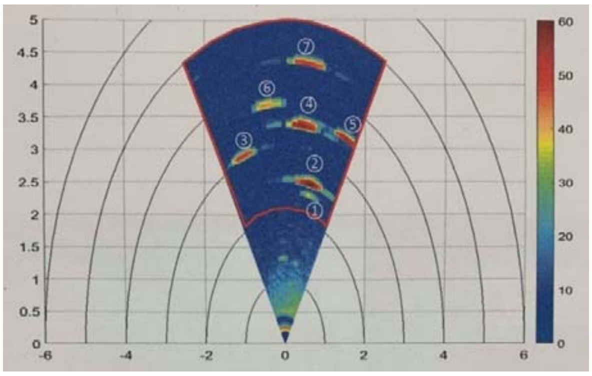

Fig. 3. The R-A map. It shows the response from the target echoes. It can be seen from the figure that there are seven ship targets. From this figure, we can see the intensity of the echo reflection of each ship target and its two-dimensional range.

Compare the information of the R-A map with the AIS, as shown in Figs. 4 (a) and (c), to find and track the ship, and input the search angle and range parameters to collect the HRRP data of the designated ship. Fourthly, execute the standby command to stop the radiation, record the HRRP data and the AIS ship information for the later recognition of the ship. Finally, repeat the above steps to collect the ship HRRP and AIS ship information. For increasing the diversity of the database, collect information on the same ship at different locations, as shown in Figs. 4 (b) and (d).

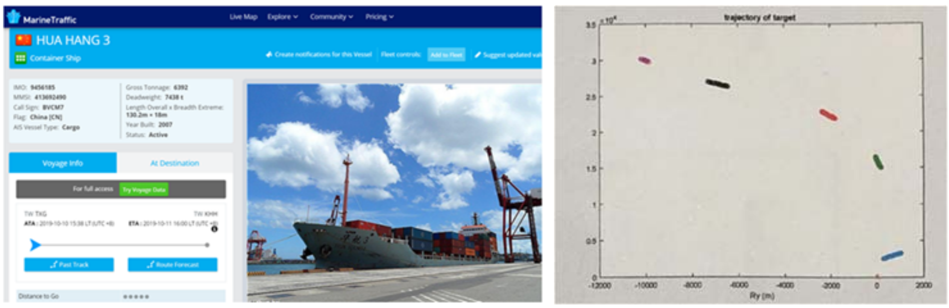

(a) (b)

Fig. 4. Some examples of AIS information and trajectories of the collected ships.

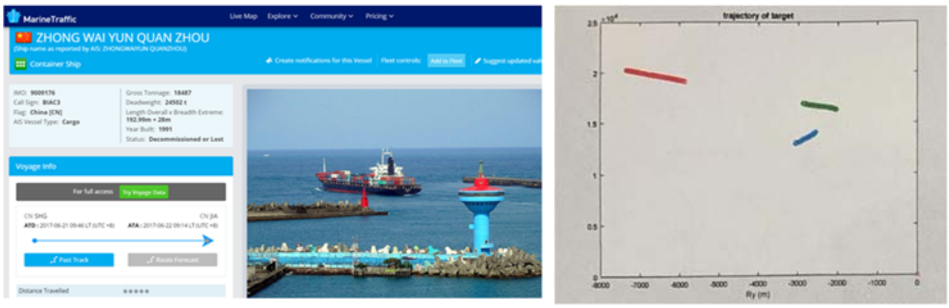

(c) (d)

Fig. 4. Some examples of AIS information and trajectories of the collected ships; (a) and (c) show the AIS information of two ships; (b) and (d) show the trajectories of the two ships shown in (a) and (c), respectively. Each different color trajectory represents a different continuous data collected. These data can indicate that the ship data collected are diverse, including different ranges and azimuths.

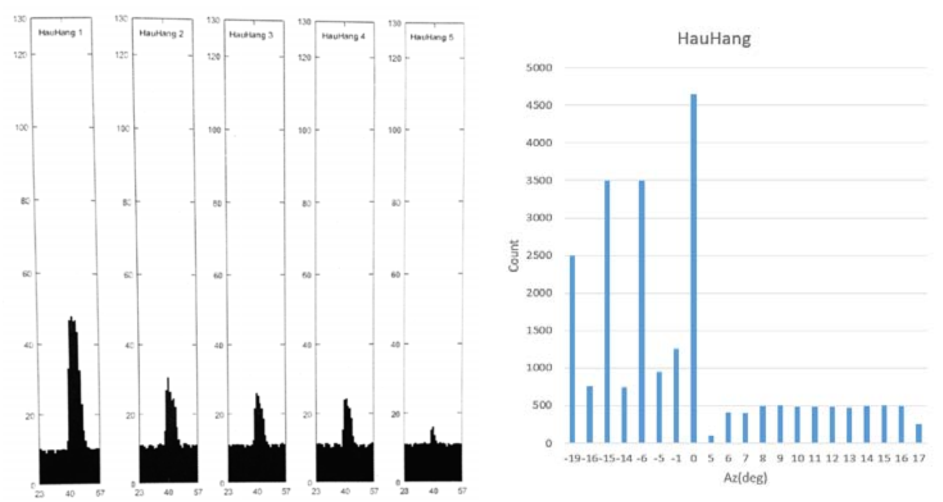

(a) (b)

Fig. 5. An example: the HRRPs of the same ship collected at different azimuth angles and its histogram; (a) shows the HRRPs of the same ship named HuaHang collected at different azimuth angles; (b) exhibits the histogram of HuaHang's HRRPs collected at different azimuth angles.

Ships in real-life are non-cooperative targets. However, the collected data sets are diverse. Fig. 5 (a) is the HRRPs of the same ship named HuaHang collected at different azimuth angles. The X axis represents the range cells from 23 to 57. The Y axis is the intensity of the target's echo. The five HRRPs from left to right in Fig. 5 (a) are the points taken from the five trajectories from right to left of Fig. 4 (b). They represent the HRRPs of the HuaHang ship at five different azimuth angles which are located at 15, 0, –6, –12, –17 angles of the azimuth respectively. Fig. 5 (a) demonstrates that the HRRPs of the same ship at different angles are slightly different. Fig. 5 (b) shows the histogram of HuaHang's HRRPs collected at different azimuth angles. The histogram exhibits that the HRRPs are collected at the azimuth angle between about −20 and 20 angles. The X axis represents the azimuth angle. The Y axis means the number of the HRRP chips collected at different azimuth angles.

This research collects a large amount of HRRP data. After the program automatically inspects the data, the original dataset has a total of 207,610 chips data, and the invalid chips data with the echo values of 0 are removed. The number of valid data after selecting is 207,545. There are six types of ships for this research. The six types of ships are named Alpha, Beta, Gamma, Delta, Epsilon, and Zeta, as shown in Fig. 6. Table 1 show the distributions of chips data. The raw data is the hexadecimal data, and the two tuples represent a decimal value, and the data byte order is little-endian.

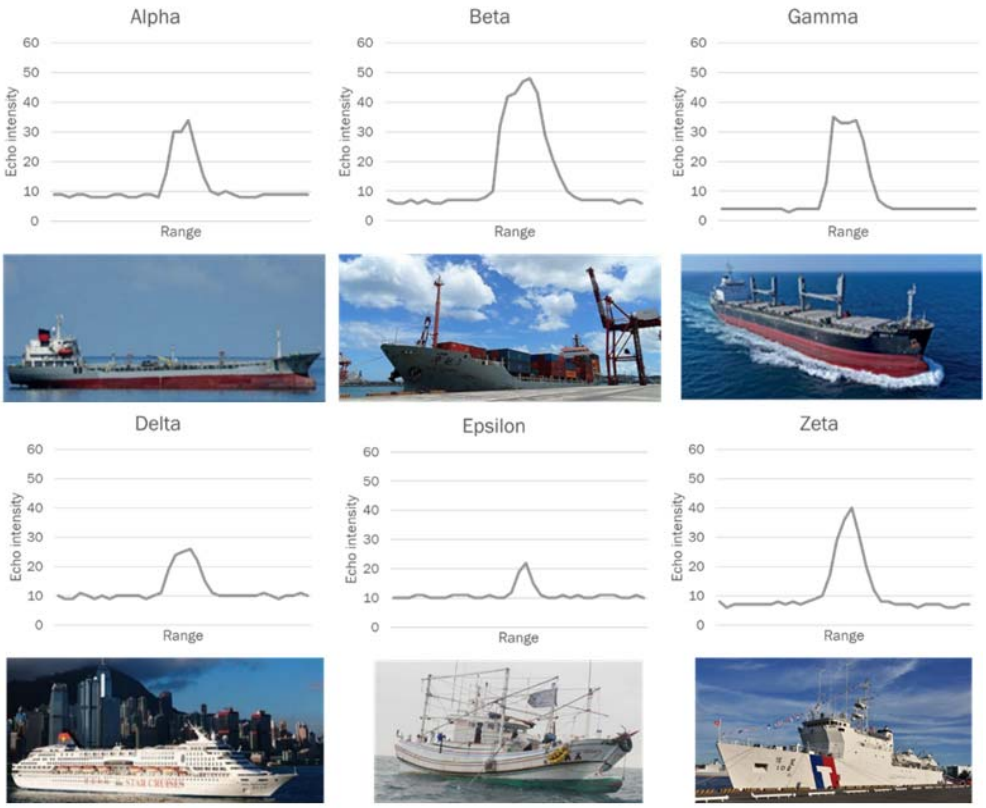

Fig. 6. Six ship types and their HRRPs.

Table 1. Six ship types and chips data distribution.

Ship type	Original chips	Valid chips
Alpha	66792	66746
Beta	40346	40344
Gamma	21697	21680
Delta	53082	53082
Epsilon	11493	11493
Zeta	14200	14200
Total	207610	207545

Fig. 7 is a schematic diagram of the hexadecimal raw data format of the original data files of the collected ships. Each file begins with the ship code, as shown in (a) for the type of ship; (b) for the ship number of the classification; (c) for the reserved field; (d) for the frame number; and (e) is a HRRP with range cell size 35.

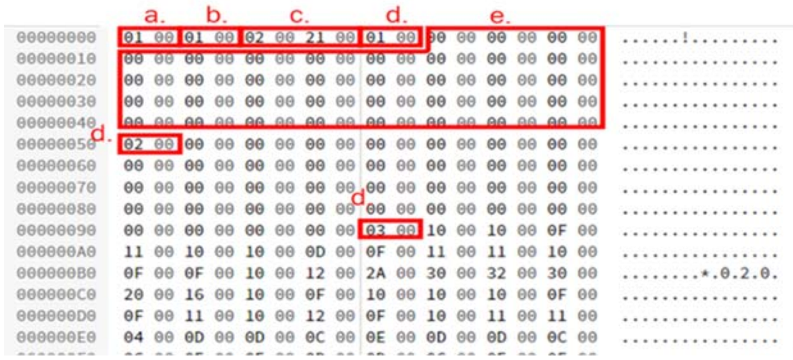

Fig. 7. The hexadecimal raw data format of the original files of the collected ships

3. PREPROCESSING

The preprocessing of HRRP plays an important role. The data format of the input network is an important factor to the effect of feature extraction. After proper preprocessing approaches, it is possible to enrich the features, thereby enhancing recognition performance.

3.1 Non-Coherent Integration

A single target echo has a lower SNR, so if the target is not large, it will not be easily detected. In addition, a single target echo causes a signal fluctuation due to the ship's movement. This can be improved by NCI. NCI is to align consecutive pules and accumulate N pules. NCI can reduce the target aspect- and amplitude-sensitivity and improve the stability of HRRP. The results from our experiments show a high recognition rate, so it can be inferred that HRRP has stable characteristics after continuous target echoes are accumulated by NCI. That is to say, HRRP collected from different aspects has stable amplitude characteristics and discriminative.

3.2 Eliminate Noisy Range Cells

The size of the ship's target usually has a certain reasonable value, so the numbers of range cell corresponding to the target echoes do not need to be observed too much when performing target recognition. In order to reduce the dimensions of the feature vector and the computational load, after aligning the center of the range cell, only reserve 35 range cells for target recognition.

3.3 Data Format Transformation

In the following sections, this research will introduce three different types of data formats based on the original data as shown in Fig. 6. The first is the one-dimensional HRRP data format, which is the most commonly used form for most papers. The second is the two-dimensional gray-scale HRRP data format proposed by [13]. The third is the proposed solution, namely two-dimensional binary-map HRRP data format.

(A) One-dimensional HRRP data format

Convert the raw data into a one-dimensional HRRP data format with labels, and take out 1×35 range cells and use them as input data for one-dimensional CNN.

(B) Two-dimensional gray-scale HRRP data format

O. Karabayır *et al.* [13] proposed stacking a one-dimensional HRRP data by just copying to obtain an enhanced performance two-dimensional gray-scale image. In this paper, the one-dimensional 1×35 HRRP will be copied and stacked into a two-dimensional gray-scale HRRP of 35×35.

(C) Two-dimensional binary-map HRRP data format

By observing the HRRP of the ship target, the radar echoes reflected by the structure of different ship targets will have different correlations, so they can be roughly classified by visual perception. Therefore, the most suitable way is to regard HRRP as two-dimensional image, as shown in Fig. 8.

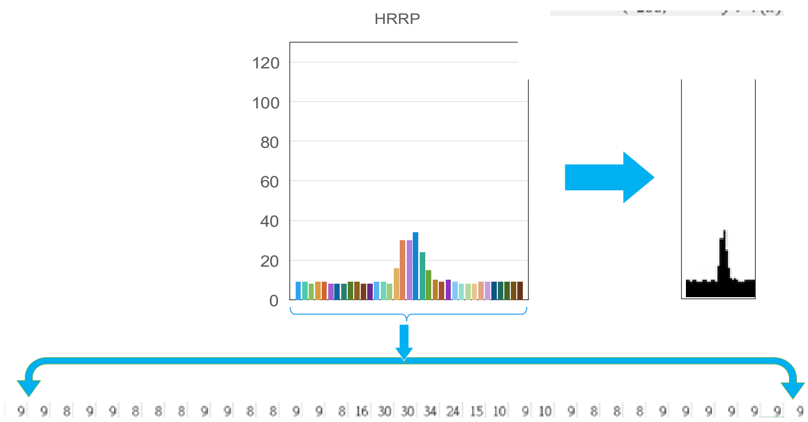

Fig. 8. Schematic diagram of the two-dimensional binary-map HRRP data format.

In this paper, a HRRP with 35 range cell is presented in a bar graph, and the image is a binary-map of size 130×35. The range cell is taken as the X-axis and the echo intensity is taken as the Y-axis of the binary image. If the echo intensity of the original data is $r(x)$, it is a real number; x is range cell number and is an integer. The value $f(x, y)$ of the pixel coordinate (x, y) defining the binary image is equal to 255 or 0; the conversion relationship between $r(x)$ and $f(x, y)$ is expressed as follows:

$$f(x,y)=\begin{cases}0, & 0\le y\le r(x)\\ 255, & y>r(x)\end{cases}. \tag{1}$$

4. DESIGN OF THE PROPOSED CNN

CNN is a popular and famous neural network for Deep Learning. It is pointed out from most of the papers that CNN was first introduced by Y. LeCun *et al.* [18] in 1995.

The proposed approach uses CNN to recognize ship targets based on radar HRRP dataset. The design of the proposed CNN starts with two convolutional layers and two fully-connected layers, as shown in Fig. 9. However, in order to avoid overfitting, the dropout layer is added, and then the number of layers of the network is gradually adjusted to find better performance. This research proposes four different CNN architectures and experiment with three input data formats under each architecture. The four CNN architectures are as follows:

1. CNN_{2C2F}: CNN consists of two convolutional layers and two fully-connected layers.
2. CNN_{2C3F}: CNN consists of two convolutional layers and three fully-connected layers.
3. CNN_{3C2F}: CNN consists of three convolutional layers and two fully-connected layers.
4. CNN_{3C3F}: CNN consists of three convolutional layers and three fully-connected layers.

The proposed CNN architectures are containing the convolutional layers with the kernel size of 5×5, stride of 1×1, padding size of 1×1, and the maxing pooling layers with the size of 2×2. The drop rate of the first layer is set to 0.25, and the remaining drop rate is 0.5.

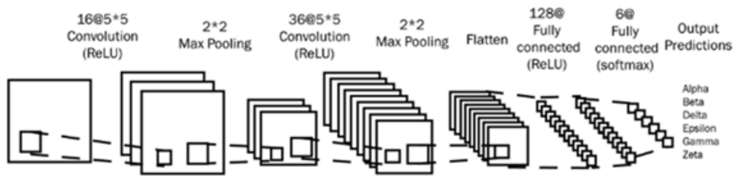

Fig. 9. The CNN architecture composed of two convolutional layers and two fully-connected layers.

4.1 Activation Function

The activation function simulates the effect of a threshold in a biological neuron. When the signal strength reaches a threshold, the signal is output, otherwise there is no output. The activation function is generally a nonlinear function, which performs nonlinear transformation on the input signal, and then passes the transformed output as input to the next layer of neurons, so that the neural network can solve more complicated problems. The equation is expressed as

$$Y = Activation(\sum(weight * input)+bias). \quad (2)$$

(A) ReLU

In the experiment, the ReLU activation function is selected. Compared with the traditional Sigmoid and Tanh, the computation amount of ReLU is small, the convergence speed is obviously faster, and the problem of gradient vanish is relatively less likely to occur. In addition, ReLU will cause the output of some neurons to be zero to sparse the neural network and avoid overfitting problems. ReLU is defined as

$$f(y) = max(0, y). \tag{3}$$

(B) Softmax

The Softmax function [19] is a generalization of logistic Regression. The basic goal of Softmax is to convert numbers into probabilities. It can normalize a K-dimensional vector with any real number into a probability distribution which consists of K probabilities proportional to the exponentials of the input numbers, so that each element function. The Softmax is defined as

$$\sigma(z)_j = \frac{e^{z_j}}{\sum_{k=1}^{K} e^{z_k}}, \quad \text{for } j = 1,\ldots,K. \tag{4}$$

4.2 Loss Function

In order to know the quality of the model training, the loss function [20] is used to evaluate the prediction result of the model; if the predicted result is too different from the actual result, the loss function will be large. With the help of some Optimizer, the loss function gradually reduces the prediction error as the model learns.

In this paper, the cross entropy is used as the loss function. Compared with other loss functions, the gradient decreases faster. However, it is worth noting that the cross entropy must be used with Softmax, and the label needs to be a one-hot type binary value sequence.

Suppose x is a random variable, $p(x)$ is a probability density function, and the information gain $I(x)$ is defined as Eq. (5). It means that the lower the probability, the larger the information gain. Entropy is the average information gain contained in all received messages. It can also be regarded as the turmoil of the data or the uncertainty of the data. The entropy equation is defined as Eq. (6).

In the classification problem, each data has a set of prediction probability, so when calculating the cross entropy of each data, the entropy calculated by each category is added, as shown in Eq. (7) [20].

$$I(x) = -\log_2(p(x)) \tag{5}$$

$$H(X) = \textstyle\sum_i - p_i \log_2(p_i) \tag{6}$$

$$H = \sum_{c=1}^{C} \sum_{i=1}^{n} -y_{c,i} \log_2(p_{c,i}) \tag{7}$$

where c is the category and n is all the number of data, $y_{c,i}$ is a binary indicator which means that the ith data belongs to the real category of the c-class. $P_{c,i}$ is the probability that the ith data belongs to the c-class prediction.

4.3 Optimizer

Use the optimizer to adjust the model's parameters during training to reduce the value of loss function and make the prediction as accurate as possible. In other words, the optimizer is actually an optimization of the gradient descent algorithm, and the optimizer will be told that it is moving in the right or wrong direction. The well-known optimizers such as RMSprop, AdaGrad and Adam have similar effects in many cases.

RMSProp optimizer learns faster when the gradient is large, and slows down when the gradient becomes smaller. AdaGrad can amplify the learning rate when the previous gradient is small, and can constrain the learning rate when the gradient is large. Adam retained RMSProp's approach of adjusting the gradient velocity in the past gradient direction and AdaGrad's adjustment of the learning rate of the past gradient squared value, and "bias-correction" of the parameters, so that each learning rate has a clear range, so that the update parameters are relatively stable. The Adam algorithm is computationally efficient and suitable for problems with large data and parameters. Adam's application to MNIST character recognition is significantly lower than other optimizers, as shown in Fig. 10 [21]. Therefore, Adam is the best choice.

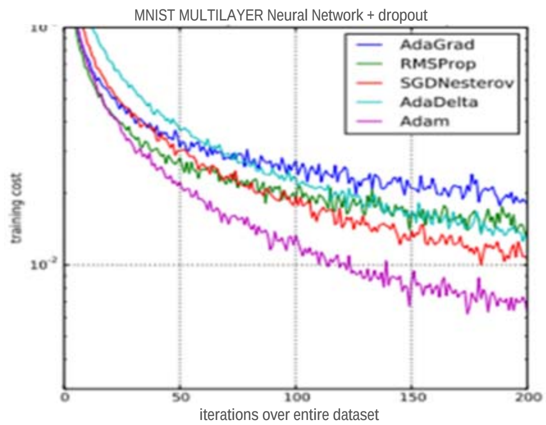

Fig. 10. Diagram of the optimizer comparison [21].

The initial learning rate is set to 0.001, and the optimizer selects Adam. In general, within a reasonable range, the larger the batch size, the more accurate the direction to the optimum. If the batch size is too large, a local optimum may occur. The small batch size introduces more randomness and will bounce around the optimum and be difficult to achieve convergence. But in rare cases, the small batch size may work better. After testing, the batch size is set to 300. As for the selection of the activation function, except that the activation function of the fully-connected layer of the last layer is Softmax for outputting the probability of each class to which the target belongs, the activation functions of the remaining layers are all Rectified Linear Units (ReLU).

5. EXPERIMENTS AND ANALYSIS

The proposed CNN is based on adjusting the convolutional layers and fully-connected layers of the CNN architecture to explore the applicability of the HRRP dataset used in CNN applied in this research. The kernel size of the convolutional layer is 5×5, and the kernel size of the max-pooling layer is 2×2.

In the experiment, 20% of the training set is used as the validation set in the training process, and the accuracy of the validation set is used to evaluate the quality of the model. The initial learning rate is set to 0.0001, and the batch size is 300. After 70% data training set experiment, the Further, Fig. 11 shows the confusion matrix of the classification results by using the two-dimensional binary-map HRRP as the test dataset. The HRRP of the Gamma ship is similar to the Alpha ship, and the number of samples of Alpha is relatively large, so the probability of 1.01% of the Gamma ship is incorrectly predicted as Alpha ship. The Epsilon ship is similar to the Delta ship's HRRP, and the Delta has a relatively large number of samples, so the Epsilon ship has a 1.63% chance of being mispredicted as a Delta ship. Recognition accuracy curves of training and testing set for three data formats are shown in Figs. 12 (a)-(c).

	Alpha	Beta	Gamma	Delta	Epsilon	Zeta
Alpha	98.05	0.27	0.47	1.08	0.03	0.1
Beta	0.32	99.51	0.03	0.02	0.07	0.03
Gamma	2.01	0.06	97.83	0.09	0	0
Delta	0.5	0.15	0.01	99.11	0.19	0.03
Epsilon	0.06	0.32	0	6.64	92.86	0.12
Zeta	0.54	0.23	0	0.35	0.09	98.78

Fig. 11. The confusion matrix of two-dimensional binary-map HRRP using CNN_{3C2F}.

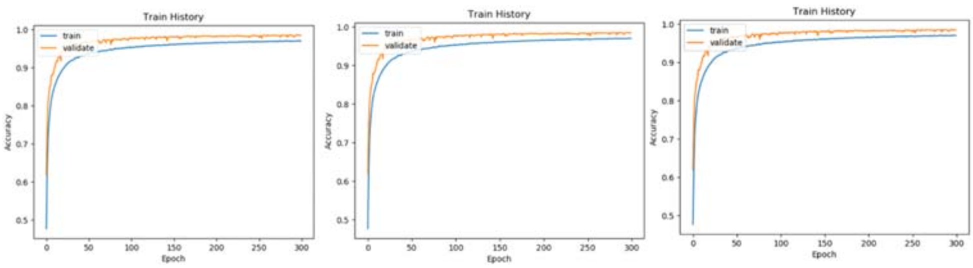

(a) (b) (c)

Fig. 12. Recognition accuracy curve of training and testing set for three data formats: (a) one-dimensional HRRP data format; (b) two-dimensional gray-scale HRRP data format; and (c) two-dimensional binary-map HRRP data format.

As shown in Fig. 12 (a), the accuracy of the validation set does not increase significantly after 250 epochs, so the epoch of the one-dimensional HRRP data format experiment is set to 300. As shown in Fig. 12 (b), the accuracy of the validation set does not increase significantly after 150 epochs, so the epoch of the two-dimensional gray-scale HRRP data format experiment is set to 200, and the accuracy of the validation set in Fig. 12 (c) does not increase significantly after 60 epochs, so the epoch of the two-dimensional binary-map HRRP data format experiment is set to 100.

In the experiments, we split the data with two manners, including in the ratio of 5:5 and 7:3, to the training and test dataset respectively. It can be seen from Tables 2-5 that the experimental results in the ratio of 7:3 for the training and test dataset are better, and the accuracy is improved by about 0.001~0.003.

In order to facilitate the comparison of the four neural network architectures and the applicability of the three data formats, the experimental results of the training data of 70% are taken as an example. It can be seen from Tables 2-5 that from the perspective of architecture adjustment, a small increase in the convolutional layer or the fully-connected layer of the CNN architecture does not significantly improve the recognition rate. From the perspective of the data format fed to the neural network, O. Karabayır *et al.* [13] proposed stacking a one-dimensional HRRP data by just copying to obtain an enhanced performance two-dimensional gray-scale image and directly feeding the one-dimensional HRRP to the neural network. The difference in recognition rate is not significant, both between 98-99%. Compared with the former two, the two-dimensional binary-map HRRP data format proposed in this paper has the best recognition rate, and can reach the recognition rate of more than 99%.

In order to meet the application requirements of real-time ship target recognition in the future, the authors have counted the test time. This paper uses a training model with a better test accuracy to count the test time, that is, the dataset of the model is divided into a training dataset and a test dataset with a ratio of 7:3. "Total" means that 62,263 chips of test data are read continuously, and "one" means that only one chip of test data is read in an experiment. The time calculated in this experiment includes the calculation of file reading, data format conversion, one-hot encoding and testing.

From Fig. 13 and Tables 2-5, it can be seen that it takes a lot of time to read only one chip of data, which takes about 6 seconds on average. The average test time obtained by reading all the test data at one time is very fast, only about 0.00023 seconds, which means that every execution most of the time for a program is to initialize the environment and read files. The size of a single test data is not the main reason for the prolonged test time.

Table 2. Network parameters and performance of CNN_{2C2F} for 3 HRRP data formats.

	one-dimensional		two-dimensional gray-scale		two-dimensional binary-map	
Epoch	300		200		100	
Parameters	40778		310666		1195402	
Train : Test data	5:5	7:3	5:5	7:3	5:5	7:3
Training time(s)	592.24	843.76	684.64	988.854	828.60	1173.98
Validation Loss	5.90%	4.24%	4.36%	4.11%	3.73%	3.39%
Validation Accuracy	98.25%	98.63%	98.57%	98.63%	99.11%	99.18%
Testing time(s) (total)	–	8.42	–	9.74	–	21.89
Testing time(s) (one)	–	6.02	–	5.77	–	5.89
Test Loss	5.87%	4.34%	5.14%	4.38%	3.04%	3.10%
Test Accuracy	98.15%	98.53%	98.27%	98.47%	99.16%	99.17%

Table 3. Network parameters and performance of CNN_{2C3F} for 3 HRRP data formats.

	one-dimensional		two-dimensional gray-scale		two-dimensional binary-map	
Epoch	300		200		100	
Parameters	48650		318538		1203274	
Train : Test data	5:5	7:3	5:5	7:3	5:5	7:3
Training time(s)	682.94	918.00	695.89	992.17	848.14	1183.43
Validation Loss	5.27%	4.50%	5.22%	4.49%	3.80%	3.50%
Validation Accuracy	98.30%	98.47%	98.31%	98.51%	99.09%	99.14%
Testing time(s) (total)	–	8.83	–	10.16	–	23.84
Testing time(s) (one)	–	6.06	–	6.20	–	5.99
Test Loss	5.32%	4.58%	5.41%	4.45%	3.30%	3.23%
Test Accuracy	98.15%	98.46%	98.12%	98.44%	99.05%	99.15%

If real-time response is emphasized in actual application, the users can choose one-dimensional HRRP data format as the input data type, and use CNN_{2C2F} as the model, in which it only takes 8.42 seconds to predict all the test data. If higher accuracy is required in actual application, the users can choose two-dimensional binary-map HRRP data format as the input data type, and use CNN_{3C2F} as the model. It takes 22.61 seconds to predict all the test data with the accuracy rate 99.20%.

Table 4. Network parameters and performance of CNN_{3C2F} for 3 HRRP data formats.

	one-dimensional		two-dimensional gray-scale		two-dimensional binary-map	
Epoch	300		200		100	
Parameters	53810		228082		670450	
Train : Test data	5:5	7:3	5:5	7:3	5:5	7:3
Training time(s)	653.61	930.79	805.65	1120.80	975.30	1350.35
Validation Loss	3.55%	3.43%	5.26%	4.14%	4.53%	3.37%
Validation Accuracy	98.89%	98.88%	98.66%	98.79%	99.07%	99.25%
Testing time(s) (total)	–	8.79	–	10.90	–	22.61
Testing time(s) (one)	–	6.30	–	6.06	–	6.25
Test Loss	3.58%	3.40%	5.16%	4.53%	3.79%	3.27%
Test Accuracy	98.82%	98.84%	98.59%	98.64%	99.07%	99.20%

Table 5. Network parameters and performance of CNN_{3C3F} for 3 HRRP data formats.

	one-dimensional		two-dimensional gray-scale		two-dimensional binary-map	
Epoch	300		200		100	
Parameters	61682		235954		678322	
Train : Test data	5:5	7:3	5:5	7:3	5:5	7:3
Training time(s)	669.04	903.25	804.37	1138.76	990.11	1361.47
Validation Loss	3.52%	2.93%	5.08%	4.85%	5.25%	3.66%
Validation Accuracy	98.91%	99.04%	98.55%	98.73%	99.06%	99.17%
Testing time(s) (total)	–	8.82	–	10.30	–	22.75
Testing time(s) (one)	–	6.61	–	6.04	–	6.10
Test Loss	3.28%	3.00%	5.16%	4.86%	4.56%	3.67%
Test Accuracy	98.89%	98.97%	98.31%	98.59%	99.10%	99.11%

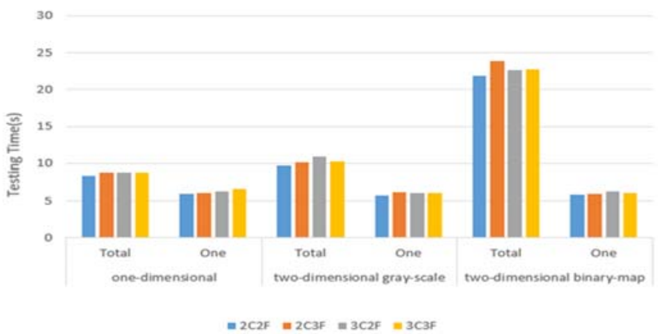

Fig. 13. Testing time for different CNN architectures with 3 HRRP data formats.

Table 6 summarizes some well-known CNN architectures compared with the proposed architecture. These well-known CNNs, including LeNet, AlexNet and ZFNet, all use our dataset and two-dimensional binary-map HRRP data format. Table 6 shows that LeNet is the most similar to our architecture, but the performance is slightly worse. The architectures of AlexNet and ZFNet are much more complicated, and they cannot achieve better recognition accuracy. Table 6 exhibits that the proposed architecture, which has three convolutional layers and two fully-connected layers, is slightly better than the other well-known architectures. Therefore, for the recognition of our dataset, a deeper network may not be able to get better results but it consumes more time.

Table 6. Comparison of different CNNs with our proposed architecture.

	LeNet	AlexNet	ZFNet	The proposed approach
Parameters	1798966	36667966	23859190	670450
Train : Test data	7:3	7:3	7:3	7:3
Training time(s)	31097.16	130881.67	21539.12	1350.35
Validation Loss	3.47%	6.20%	4.56%	3.37%
Validation Accuracy	99.09%	99.04%	98.95%	99.25%
Testing time(s) (total)	63.85	349.79	66.48	22.61
Test Loss	3.53%	5.99%	4.78%	3.27%
Test Accuracy	99.05%	98.94%	98.85%	**99.20%**

Table 7 summaries classification results of some published papers. In Table 7, the datasets in the [11-13, 15, 16] studies are all established in a simulated manner, and the datasets used in our experiments are the data collected in the real-life situation.

There are relatively few studies using deep learning on the HRRP target recognition. Most of the HRRP data of the researches are generated in a simulated way, rather than the data collected under the real-life environment. Therefore, it is difficult to be applied in real-world conditions to recognize the ship.

From Table 7, it can be found that the accuracy of the research using the neural network to identify the ship is better than the result of using the traditional approach. It also demonstrates the proposed approach is comparable to the other state-of-the-art HRRP target recognition approaches.

Table 7. Comparison of different approaches for HRRP recognition performance.

Approach	Dataset	Description	Recognition accuracy(%)
[11]	Simulation data	FMT, SVM	80%
[12]	Simulation data	Frame segmentation, Bayes	89.36%
[13]	Simulation data	MatConvNet	93.90%
[15]	Simulation data	CNN-ELM	99.50%
[16]	Simulation data	CNN-BiRNN	93.30%
One-dimensional HRRP With our dataset	Real-life data	CNN_{3C2F}	98.84%
[13] with our dataset	Real-life data	CNN_{3C2F}	98.64%
The proposed approach	Real-life data	CNN_{3C2F}	**99.20%**

Bold values indicate the best performance with real-life data.

6. CONCLUSIONS

This research constructs a ship radar HRRP dataset with the radar and AIS, and proposed a CNN-based ship target recognition approach experimenting with this dataset. First, this paper describes how to build a real-life HRRP dataset of ship targets. Then, preprocessing approaches for the ship HRRP dataset are described. After that, three different HRRP data format are proposed, including the common one-dimensional HRRP data format, the two-dimensional gray-scale HRRP data format proposed in [13], and the two-dimensional binary-map HRRP data format proposed by us are introduced. Furthermore, we have designed four different architectures of CNN to compare the recognition performance of the above three data formats by adjusting the number of network layers. Finally, experimental results showed that the proposed approach has a brilliant performance for recognition.

The proposed approach has three key advantages: (1) Experiments with ship HRRP datasets collected by using radar and AIS from actual coastline in this research are more realistic than most other papers using simulated datasets; (2) The proposed two-dimensional binary-map HRRP data format has better recognition performance than other data formats, so it can be known that the appropriate data preprocessing can improve the recognition accuracy; (3) In this research, the experimental results show that the proposed approach based on CNN architecture can prove that CNN can automatically learn the discriminant deep features of HRRP. It is feasible to use CNN to automatically classify ship targets based on HRRPs.

The result of the proposed approach is comparable to the other state-of-the-art HRRP target recognition approaches. Through the experiments in this research, it is proved that it is feasible and high-accuracy to use CNN to recognize the ship target based on HRRPs collected from the actual coastline. The findings of this research help to extend HRRP recognition technology to coastal surveillance and military radar automatic target recognition.

ACKNOWLEDGEMENT

The authors would like to acknowledge the support for this research through grants from Ministry of Science and Technology (MOST 109-2637-E-146-001). They would also thank the anonymous reviewers for their significant and constructive critiques and suggestions, which substantially improved the quality of this paper.

REFERENCES

1. H.-J. Li and S.-H. Yang, "Using range profiles as feature vectors to identify aerospace objects," *IEEE Transactions on Antennas and Propagation*, Vol. 41, 1993, pp. 261-268.
2. Y. Wang, Y. Jiang, Y.-H. Wang, Y. Li, and J. Xu, "Scattering center estimation of HRRP via atomic norm minimization," in *Proceedings of International Conference on IEEE Radar*, 2017, pp. 135-139.
3. D. Zhou, X. Shen, and W. Yang, "Radar target recognition based on fuzzy optimal

transformation using high-resolution range profile," *Pattern Recognition Letters*, Vol. 34, 2013, pp. 256-264.
4. J. Liu, N. Fang, Y.-J. Xie, and B.-F. Wang, "Multi-scale feature-based fuzzy-support vector machine classification using radar range profiles," *IET Radar*, *Sonar and Navigation*, Vol. 10, 2016, pp. 370-378.
5. D. Zhou, "Radar target HRRP recognition based on reconstructive and discriminative dictionary learning," *Signal Processing*, Vol. 126, 2016, pp. 52-64.
6. L. Du, H. He, L. Zhao, and P.-H. Wang, "Noise robust radar HRRP targets recognition based on scatterer matching algorithm," *IEEE Sensors Journal*, Vol. 16, 2016, pp. 1743-1753.
7. A. Zyweck and R. E. Bogner, "Radar target classification of commercial aircraft," *IEEE Transactions on Aerospace and Electronic Systems*, Vol. 32, 1996, pp. 598-606.
8. J. Lundén and V. Koivunen, "Deep learning for HRRP-based target recognition in multistatic radar systems," in *Proceedings of IEEE Radar Conference*, 2016, pp. 1-6.
9. B. Pei and Z. Bao, "Multi-aspect radar target recognition method based on scattering centers and HMMs classifiers," *IEEE Transactions on Aerospace and Electronic Systems*, Vol. 41, 2005, pp. 1067-1074.
10. B. Feng, B. Chen, and H. Liu, "Radar HRRP target recognition with deep networks," *Pattern Recognition*, Vol. 61, 2017, pp. 379-393.
11. J. Lu, Z. Xi, X. Yuan, G. Yu, and M. Zhang, "Ship target recognition using high resolution range profiles based on FMT and SVM," in *Proceedings of IEEE CIE International Conference on Radar*, 2011, pp. 1299-1302.
12. J. Lu, S. Tian, and Z. Xi, "Frame segmentation and recognition algorithm for ship's HRRPs based on hypothesis testing," in *Proceedings of CIE International Conference on Radar*, 2016, No. 2016.8059572.
13. O. Karabayır, O. M. Yücedağ, M. Z. Kartal, and H. A. Serim, "Convolutional neural networks-based ship target recognition using high resolution range profiles," in *Proceedings of International Radar Symposium*, 2017, No. 2017.8008207.
14. J. Song, Y. Wang, W. Chen, Y. Li, and J. Wang, "Radar HRRP recognition based on CNN," *The Journal of Engineering*, Vol. 2019, 2019, pp. 7766-7769.
15. Q. Zhang, J. Lu, T. Liu, P. Zhang, and Q. Liu, "Ship HRRP target recognition based on CNN and ELM," in *Proceedings of International Conference on Electromechanical Control Technology and Transportation*, 2019, No. 2019.00035.
16. J. Wan, B. Chen, Y. Liu, H. Liu, and L. Jin, "Recognizing the HRRP by combining CNN and BiRNN with attention mechanism," *IEEE Access*, Vol. 8, 2020, pp. 20828-20837.
17. T.-P. Chen, C.-L. Lin, K.-C. Fan, W.-Y. Lin, and C.-W. Kao, "Apply convolutional neural network to radar automatic target recognition based on real-life radar high-resolution range profile of ship target," in *Proceedings of the 33rd IPPR Conference on Computer Vision*, *Graphics*, *and Image Processing*, 2020, No. 72487.
18. Y. LeCun and Y. Bengio, "Convolutional networks for images, speech, and time series," *The Handbook of Brain Theory and Neural Networks*, MIT Press, MA, 1995, pp. 1-14.
19. Softmax function, https://en.wikipedia.org/wiki/Softmax_function, 2020.
20. R. Parmar, "Common Loss functions in machine learning," https://towardsdatascience.com/common-loss-functions-in-machine-learning-46af0ffc4d23.

21. D. P. Kingma and J. Ba, "Adam: A method for stochastic optimization," in *Proceedings of International Conference for Learning Representations*, 2015, pp. arXiv: 1412. 6980

Tsung-Pin Chen (陳宗斌) received his B.S. and M.S. degrees in Computer Science and Information Engineering from National Central University, Taiwan, in 1997 and 1999, respectively. He is currently pursuing his Ph.D. degree in the same department at the same university since September 2016. He is also an Associate Researcher at the National Chung-Shan Institute of Science and Technology (NCSIST). His research interests include biometrics, radar target recognition, pattern recognition, and machine learning.

Chih-Lung Lin (林志隆) received his Ph.D. from the Institute of Computer Science and Information Engineering at National Central University in 2003. From 1989 to 2007, he was an Assistant Researcher at the National Chung-Sun Institute of Science and Technology (NCSIST), Taiwan, where he became a project manager in 1994. He joined the Hwa Hsia Institute of Technology as an Assistant Professor in the Department of EE in 2009 and became an Associate Professor and a Professor in 2011 and 2016, respectively. He was the Chairman of EE Department in Hwa Hsia University of Technology from 2016 to 2017. Currently, he is the chairman of Bachelor Degree Program of Robotics, Graduate Institute of Intelligent Robotics and the Dean of Information Technology and Engineering college in Hwa Hsia University of Technology. Professor Lin has also received some awards, including 2012 Excellent Mentor Award, 2013 and 2018 Excellent Faculty Award and 2018 Excellent Researcher Project Award from Hwa Hsia University of Technology. He also serves as reviewers in many prominent international journals, including IEEE Transactions on Information Forensics & Security, Information Sciences, IET Computer Vision, *etc.* His current research interests include biometrics verification, artificial intelligence (AI), pattern recognition, and image processing.

Kuo-Chin Fan (范國清) was born in Hsinchu, Taiwan in 1959. He received the B.S. degree in Electrical Engineering from National Tsing Hua University, Hsinchu, Taiwan in 1981, and the M.S. and Ph.D. degrees from the University of Florida (UF), Gainesville, in 1985 and 1989, respectively. He then joined the Institute of Computer Science and Information Engineering, National Central University, Taiwan, where he became a professor in 1994. He was the Chairman of the Department from 1994 to 1997 and the Vice President of Fo-Gung university from 2007 to 2011. Currently, he is the Chair Professor of Institute of Computer Science and Information

Engineering in National Central University and the Dean of Computer Science and Electrical Engineering College, Taiwan. He received three consecutive Distinguished Research Fellow Awards from National Science Council and was appointed Life Distinguished Research Fellow in 2011. His research interests include image analysis, biometric verification, and video surveillance.

Wan-Yu Lin (林宛諭) received the B.S degree in Software Engineer and Management from National Kaohsiung Normal University, Kaohsiung, Taiwan in 2017, and the M.S degree in Computer Science and Information Engineering from National Central University, Taoyuan, Taiwan in 2019. Currently, she is an Engineer at HP International Pte. Ltd., Taiwan Branch. She is responsible for analyzing work efficiency of company members. Her research interests include machine learning, image analysis, text mining, and data analysis.

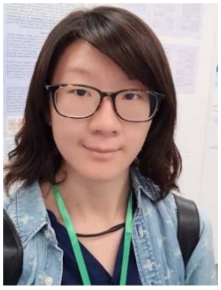

Chiao-Wen Kao (高巧汶) received the B.S. and M.S. degrees in Computer Communication and Engineering from Ming Chuan University, Taiwan, and the Ph.D. degree from the Department of Computer Science and Information Engineering, National Central University, Taiwan, in 2018. She is currently an Assistant Professor with the Department of Economics and Finance, Ming Chung University, Taiwan. Her research interests include pattern recognition, image processing, artificial intelligence and interactive media.